

# The number of corner polyhedra graphs

Clément Dervieux<sup>1†</sup>, Dominique Poulalhon<sup>1†</sup>, and Gilles Schaeffer<sup>2‡</sup>

<sup>1</sup> IRIF, Université Paris Diderot, Paris, France

<sup>2</sup> LIX, CNRS, École Polytechnique, France

---

**Abstract.** Corner polyhedra were introduced by Eppstein and Mumford (2014) as the set of simply connected 3D polyhedra such that all vertices have non negative integer coordinates, edges are parallel to the coordinate axes and all vertices but one can be seen from infinity in the direction  $(1, 1, 1)$ . These authors gave a remarkable characterization of the set of corner polyhedra graphs, that is graphs that can be skeleton of a corner polyhedron: as planar maps, they are the duals of some particular bipartite triangulations, which we call hereafter corner triangulations.

In this paper we count corner polyhedral graphs by determining the generating function of the corner triangulations with respect to the number of vertices: we obtain an explicit rational expression for it in terms of the Catalan generating function. We first show that this result can be derived using Tutte’s classical compositional approach. Then, in order to explain the occurrence of the Catalan series we give a direct algebraic decomposition of corner triangulations: in particular we exhibit a family of *almond triangulations* that admit a recursive decomposition structurally equivalent to the decomposition of binary trees. Finally we sketch a direct bijection between binary trees and almond triangulations. Our combinatorial analysis yields a simpler alternative to the algorithm of Eppstein and Mumford for endowing a corner polyhedral graph with the cycle cover structure needed to realize it as a polyhedral graph.

**Résumé.** Eppstein et Mumford (2014) ont défini l’ensemble des polyèdres en coin comme l’ensemble des polyèdres 3D dont les sommets sont à coordonnées entières positives, les arêtes sont parallèles aux axes de coordonnées et tous les sommets sont visibles depuis l’infini dans la direction  $(1, 1, 1)$ . Ils décrivent l’ensemble des graphes de polyèdres en coin, *i.e.* des graphes squelettes d’un polyèdre en coin : vus comme cartes planaires, il s’agit des graphes duaux de certaines triangulations bicoloriées particulières, que nous appelons triangulations en coin enracinées.

Dans le présent article nous comptons les graphes de polyèdres en coin en déterminant la série génératrice des triangulations en coin enracinées selon leur nombre de sommets : nous en obtenons une expression explicite en fonction de la série génératrice des nombres de Catalan. Ce résultat découle de la méthode de composition de Tutte mais pour expliquer l’apparition des nombres de Catalan, nous donnons aussi une décomposition algébrique des triangulations en coin : en particulier nous mettons en évidence une famille de triangulations en amande qui admet une décomposition structurellement équivalente à celle des arbres binaires. Pour finir nous présentons rapidement une bijection directe entre les arbres binaires et ces triangulations en amande. Notre analyse combinatoire conduit à un algorithme plus simple que celui d’Eppstein et Mumford pour munir un graphe de polyèdre en coin d’une couverture par cycles permettant de le réaliser effectivement comme polyèdre en coin.

**Keywords.** Bijection, triangulations, binary trees, Catalan numbers

---

<sup>†</sup>Emails: [Clement.Dervieux, Dominique.Poulalhon]@liafa.univ-paris-diderot.fr

<sup>‡</sup>Email: Gilles.Schaeffer@lix.polytechnique.fr

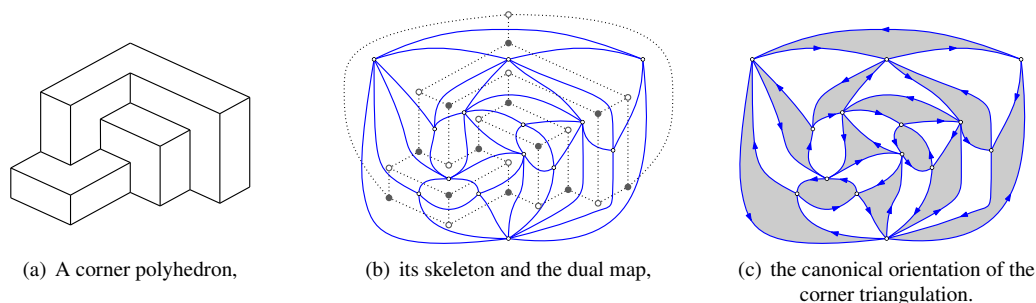


**Fig. 1:** Eppstein and Mumford's theorem

## 1 Introduction

In the recent paper Eppstein and Mumford (2014), the authors introduced and characterized a new family of 3D polyhedra: a polyhedron  $\mathcal{P}$  in  $\mathbb{R}^3$  is a *corner polyhedron* if  $v_0 = (0, 0, 0)$  is a vertex of  $\mathcal{P}$ , and:

- the boundary of  $\mathcal{P}$  has the topology of the 2-sphere,
- each edge of  $\mathcal{P}$  is parallel to one of the coordinate axis,
- exactly 3 edges of  $\mathcal{P}$  meet at each vertex,
- all vertices of  $\mathcal{P}$  but  $s$  are visible from infinity in the direction  $(1, 1, 1)$ .

By definition  $v_0$  has three neighbors  $v_1, v_2$  and  $v_3$  respectively along the  $x, y$  and  $z$  coordinate axes, and more generally all vertices of  $\mathcal{P}$  have degree 3. Recall that a *planar map* is an embedding of a graph on the sphere, considered up to orientation preserving homeomorphisms of the sphere. The skeleton of  $\mathcal{P}$  can be viewed as embedded on the boundary sphere of  $\mathcal{P}$ , and up to such homeomorphisms it is thus a cubic (or 3-regular) planar map  $P$ , which we canonically consider as rooted on the edge  $(v_0, v_1)$ . Equivalently  $P$  can be viewed as the projection of the part of the skeleton of  $\mathcal{P}$  visible from infinity on a plane with normal direction  $(1, 1, 1)$ , completed by a root vertex connected to the  $v_i, i = 1, 2, 3$  in the only possible planarity preserving way.

The starting point of our paper is Eppstein and Mumford's analog of the celebrated Steinitz's theorem for corner polyhedra. Recall that the classical Steinitz's theorem states that the set of graphs that are the skeleton of a convex polyhedron is exactly the set of 3-connected planar graphs. In order to state the analogous result for corner polyhedra, let us give some definitions. An *Eulerian triangulation* is a planar map with black and white triangular faces, such that adjacent faces have different colors. It is *rooted* if one of its edges is marked. This edge is called the *root edge*, and the incident white face the *root face*. Each edge may be canonically oriented with the incident white face on its right hand side. By convention we always use the root face as unbounded face to represent a planar map in the plane, and we classify oriented cycles in a rooted planar map as clockwise or counterclockwise accordingly. A rooted Eulerian triangulation is a *corner triangulation* if it has no double edge and the only clockwise triangles are the boundaries of the white inner faces. Finally recall that the dual of a planar map  $M$  is the map  $M^*$  obtained by putting a vertex in each face of  $M$  and a dual edge across each edge of  $M$ . Then, as illustrated in Fig. 1:

**Theorem 1 (Eppstein and Mumford (2014))** *A rooted planar map is the skeleton of some corner polyhedron if and only if its dual map is a corner triangulation.*

This neat characterization raises the question of whether it could be possible to actually count the rooted graphs that can be skeletons of corner polyhedra by counting these corner triangulations. There is indeed a long tradition of map enumeration going back to W.T. Tutte in the sixties Tutte (1962) (see also Schaeffer (2015)). However, to the best of our knowledge, the family of corner triangulations has not been considered yet.

In this paper we prove the following theorem:

**Theorem 2** *The generating series  $E^c(z)$  of corner triangulations with respect to their number of black faces is algebraic of degree 2 over  $\mathbb{Q}(t)$ . Moreover if  $A(z)$  denotes the generating function of Catalan numbers, that is, the unique formal power series solution of the equation  $A(z) = 1 + zA(z)^2$ , then*

$$E^c(z) = \frac{z(1 + 2zA(z))}{(1 + z)^3} (1 + z - z^2A(z)^2). \tag{1}$$

Equivalently, the series of corner triangulations with a marked inner white triangle is

$$E_{\Delta}^c(z) = z^2 \frac{\partial}{\partial z} \frac{E^c(z)}{z} = \frac{3z^4 A(z)^2 (1 + 2zA(z))}{(1 + z)^4}. \tag{2}$$

An explicit double summation formula for the number of corner triangulations with  $n$  black triangles can be routinely derived from the expressions of  $E^c$  above but it is not very enlightling. The first part of the statement is not so surprising, as many natural families of rooted planar maps are known to have algebraic generating functions since the early papers of Tutte (see Banderier et al. (2000) for a partial list). Indeed our first proof of Theorem 2 is based on Tutte’s compositional method, a technique already present in Tutte (1962).

More surprising is the fact that Theorem 2 directly involves the generating function of Catalan numbers. In fact a main contribution of our paper is to give a convincing interpretation of this fact. For this we introduce a new family of maps which are exactly counted by Catalan numbers. Let a *corner quasi-triangulation* be a rooted planar map without bridges nor multiple edges, whose non-root faces are black or white triangles such that adjacent triangles have different colors, and all canonically oriented clockwise triangles are the boundaries of the white faces. Then a corner quasi-triangulation  $\mathfrak{a}$  with root vertex  $s$  and a marked vertex  $t$  is an *almond triangulation* if there is a non-negative integer  $\ell$  such that the boundary of the outer face of  $\mathfrak{a}$  consists of a counterclockwise path from  $s$  to  $t$  of length  $\ell$  that is the unique shortest oriented path in  $\mathfrak{a}$  from  $s$  to  $t$ , and a clockwise path from  $s$  to  $t$  of length  $\ell + 3$ . Our interest in almond triangulations arises from the fact that they admit a decomposition structurally equivalent to the standard decomposition of binary trees. In particular we prove:

**Theorem 3** *The generating series of almond triangulations with respect to the number of black faces is the unique formal power series solution of the equation*

$$A(z) = 1 + zA(z)^2.$$

Equivalently the number of almond triangulations with  $n$  black triangles is the  $n$ th Catalan number.

Our almond triangulations are very much reminiscent of the slices of Bouttier and Guitter (2014): indeed almond triangulations exactly play regarding corner triangulations the role played in that article by  $d$ -irreducible 1-slices regarding (non-bipartite)  $d$ -irreducible triangulations. Building further on the

analogy with Bouttier and Guitter (2014), we introduce *slices* of height  $p$ , which play regarding corner triangulations the role of the 0-slices of type  $p/p + 1$  regarding  $d$ -irreducible triangulations. Two combinatorial decompositions of these slices allow us to express the generating function  $S(z)$  of all slices and the generating function  $S^+(z)$  of slices of height at least 2 in terms of  $A(z)$ :

$$(1+z)(1+S(z)) = 1+2zA(z), \quad (3)$$

$$(1+z)^2S^+(z) = z^2A(z)^2(1+2zA(z)). \quad (4)$$

At this point one possibility is to prove a pointing formula: indeed, corner triangulations with a marked white face (with generating function  $z^2 \frac{\partial}{\partial z} \frac{E^c(z)}{z}$ ) can be identified up to translation to the fundamental domains of their infinite coverings (with generating function say  $F(z)$ ), giving the relation

$$z^2 \frac{\partial}{\partial z} \frac{E^c(z)}{z} = 3F(z), \quad (5)$$

and these fundamental domains can be decomposed in terms of slices of height at least 2 to get the relation

$$(1+z)^2F(z) = z^2S^+(z), \quad (6)$$

which together with Formula (4) gives a combinatorial explanation of Formula (2). We omit here these developments for they are similar in spirit to Section 7 in Bouttier and Guitter (2014) (although some details significantly differ).

We offer instead a direct combinatorial explanation of the fact that  $E^c(z)$  is rational in  $A(z)$ : indeed a simple combinatorial argument allows us to relate corner triangulations to slices of height 1, whose generation function is simply  $S(z) - S^+(z)$ , leading to:

$$(1+z)E^c(z) = z(1+S(z) - S^+(z)). \quad (7)$$

Together with Formulas (3)–(4), this relation gives a combinatorial explanation of Formula (1) in Theorem 2. We believe that a similar direct relation between slices of bounded height and “complete objects”, which does not appear in Bouttier and Guitter (2014), should hold as well in the context of (non-bipartite)  $d$ -irreducible triangulations and quadrangulations.

Finally, we return to Theorem 3 to give a simple direct bijective correspondence between binary trees and almond triangulations in the style of the earlier bijective proofs given by the last two authors for many families of planar maps. In particular, given a binary tree our bijection constructs an almond triangulation endowed with a certain canonical orientation. We stress here that, to the best of our knowledge, this new bijection is not a known special case of the master theorems of Albenque and Poulalhon (2015); Bernardi and Fusy (2012a,b, 2014) and rather suggests that the theory still can be extended further.

**Organization of the paper.** In Section 2 we sketch the direct application of Tutte’s compositional method. Section 3 starts with a gluing lemma. In the second subsection, Theorem 3 is proved through a recursive decomposition of almond triangulations that has the same structure as the standard decomposition of binary trees. The third and fourth subsections are dedicated to the description of the decompositions of slices of arbitrary height, and of slices of height at least 2, here only stated with sketch of proofs. The fifth subsection contains the proof of Formula (7), while as announced the proofs of Formulas (5) and (6) are omitted. Finally in Section 4 we describe our direct bijection between binary trees and almond triangulations. This is an extended abstract, full detail will appear elsewhere.

## 2 Tutte’s compositional approach

Let  $\mathcal{E}$  denote the set of Eulerian triangulations,  $\mathcal{E}^s$  the subset of Eulerian triangulations without multiple edges, that is, the set of *simple Eulerian triangulations*, and  $\mathcal{E}^c$  the subset of simple Eulerian triangulations such that each clockwise triangle bounds a white face, that is, the set of *corner triangulations*.

The *size* of any Eulerian triangulation or quasi-triangulation  $\mathfrak{t}$  is the number of its black triangles, denoted by  $n(\mathfrak{t})$ . Accordingly, let  $E(x) = \sum_{\mathfrak{t} \in \mathcal{E}} x^{n(\mathfrak{t})}$  denote the generating function of Eulerian triangulations. Eulerian triangulations are dual to bicubic planar maps, so this series is well known since Tutte’s work in the sixties:

**Proposition 4 (Tutte 1964)** *The series  $E(x)$  is algebraic of degree 2 and can be expressed as*

$$E(x) = B(x) - B(x)^2$$

where  $B(x)$  is the unique formal power series solution of the equation  $B(x) = x(1 + 2B(x))^2$ .

In particular a nice explicit formula for the number of Eulerian triangulations of size  $n$  can be derived from this expression using Lagrange inversion theorem.

Tutte’s compositional approach leads to a relation between the series  $E(x)$  and  $E^s(y) = \sum_{\mathfrak{t} \in \mathcal{E}^s} y^{n(\mathfrak{t})}$ :

**Proposition 5** *The series  $E(x)$  and  $E^s(y)$  satisfy*

$$E(x) = E^s(x(1 + E(x))^3).$$

We skip here the proof of this relation as the approach is a direct adaptation of Tutte’s method: each triangulation in  $\mathcal{E}$  is decomposed into a maximal root component without multiple edges (thus an element of  $\mathcal{E}^s$ ), each edge of which is possibly sliced into a double edge to accommodate a triangulation in  $\mathcal{E}$ . A detailed presentation of the method (applied to other families of maps) is given for example in Goulden and Jackson (1983)[Chap. 2.9.12-13] or more recently in Schaeffer (2015)[Chap. 5.4.4].

Upon making the change of variable  $y = x(1 + E(x))^3$  we obtain:

**Corollary 6** *The series  $E^s(y)$  is algebraic of degree 7 and can be expressed as*

$$E^s(y) = C(y) - C(y)^2$$

where  $C(y)$  is the unique formal power series solution of the equation  $C(y) = y \frac{(1 + 2C(y))^2}{(1 + C(y) - C(y)^2)^3}$ .

In particular the first few terms in the expansion of  $E^s(y)$  are  $E^s(y) = y + y^4 + 3y^6 + 7y^7 + 15y^8 + 63y^9 + O(y^{10})$ .

Now Tutte’s compositional approach leads to a relation between  $E^s(y)$  and  $E^c(z) = \sum_{\mathfrak{t} \in \mathcal{E}^c} z^{n(\mathfrak{t})}$ :

**Proposition 7** *The series  $E^s(y)$  and  $E^c(z)$  satisfy*

$$E^s(y) = \frac{y}{E^s(y)} E^c(E^s(y)).$$

Again the proof is a fairly simple adaptation of Tutte’s method: each simple triangulation in  $\mathcal{E}^s$  is decomposed as a maximal root component without non facial clockwise triangles (thus an element of  $\mathcal{E}^c$ ), each white triangle of which is filled with a simple triangulation in  $\mathcal{E}^s$ .

Upon making the change of variable  $z = E^s(y)$  we obtain:

**Corollary 8** *The series  $E^c(z)$  is algebraic of degree 2 and can be expressed as*

$$E^c(z) = \frac{D(z) (1 - D(z))^2 (1 + 2D(z))^2}{(1 + D(z) - D(z)^2)^3}.$$

where  $D(z)$  is the unique formal power series solution of the equation  $D(z) = z + D(z)^2$ .

In particular Theorem 2 is a mere reformulation of this corollary with  $D(z) = zA(z)$ . The first few terms in the expansion of  $E^c(z)$  are  $E^c(z) = z + z^4 + 3z^6 + 4z^7 + 15z^8 + 39z^9 + O(z^{10})$ .

### 3 Algebraic decompositions

#### 3.1 Elementary properties of corner quasi-triangulations and a gluing lemma

Let us first collect some useful elementary properties of corner quasi-triangulations. Recall that the edges are canonically oriented so that they have a black face (or the root face) on the left hand side and a white face (or the root face) on the right hand side. In particular the boundary of a black triangle is a counterclockwise cycle, the boundary of a white triangle is a clockwise cycle, and each edge belongs to an oriented cycle: this implies that any corner quasi-triangulation  $\mathfrak{t}$  is strongly connected and there is an oriented path from the root vertex  $s$  to any vertex of  $\mathfrak{t}$ . Moreover any simple oriented cycle in  $\mathfrak{t}$  can be decomposed as the symmetric difference of a set of non-root faces of  $\mathfrak{t}$ ; hence the length of any oriented cycle is a multiple of 3, and so does the difference of length of any two paths with same origin and endpoint. *From now on we write path for oriented path as all the path we consider will be oriented paths. In particular, shortest path always stands for shortest oriented path.*

Now corner quasi-triangulations are characterized among quasi-triangulations with bicolored inner faces by the fact that they have no multiple edges nor non facial clockwise triangles. We state a simple condition that allows to preserve these properties while gluing two corner quasi-triangulations along their boundaries:

**Lemma 9** *Let  $\ell$  be a positive integer and consider two corner quasi-triangulations  $\mathfrak{t}_i$ ,  $i = 1, 2$ , each having two marked vertices  $s_i$  and  $t_i$  incident to the root face, and such that the shortest paths from  $s_i$  to  $t_i$  in  $\mathfrak{t}_i$  have length  $\ell$ , for  $i = 1, 2$ . Assume moreover that:*

- $\mathfrak{t}_1$  is not a single counterclockwise triangle, and the one and only shortest path  $\gamma_1$  from  $s_1$  to  $t_1$  in  $\mathfrak{t}_1$  follows the root face, with this face on its right: we call this path the right boundary of  $\mathfrak{t}_1$ .
- An oriented path  $\gamma_2$  of length  $\ell$  from  $s_2$  to  $t_2$  follows the root face of  $\mathfrak{t}_2$ , with this face on its left: we call this path the left boundary of  $\mathfrak{t}_2$ .

*Then the map  $\mathfrak{t}$  obtained by identifying the right boundary  $\gamma_1$  of  $\mathfrak{t}_1$  and the left boundary  $\gamma_2$  of  $\mathfrak{t}_2$  is a corner quasi-triangulation. Moreover the path  $\gamma$  arising from the identification of  $\gamma_1$  and  $\gamma_2$  is the leftmost shortest path between the identified vertices  $s$  and  $t$  in  $\mathfrak{t}$ .*

**Proof (sketch):** First we prove that  $\mathfrak{t}$  is a quasi-triangulation and its inner faces are well bicolored: the only new inner edges – edges of  $\gamma$  – have a black face on their left hand side (as in  $\mathfrak{t}_1$ ) and a white face on their right hand side (as in  $\mathfrak{t}_2$ ).

Then we prove that  $\mathfrak{t}$  has no double edges: since  $\mathfrak{t}_1$  and  $\mathfrak{t}_2$  have no double edges, a double edge in  $\mathfrak{t}$  should consist of two inner edges  $e_i$  from  $\mathfrak{t}_i$ , for  $i = 1, 2$ , each with both endpoints on  $\gamma_i$ . But the existence of  $e_1$  would prevent  $\gamma_1$  from being the only shortest path from  $s_1$  to  $t_1$ .

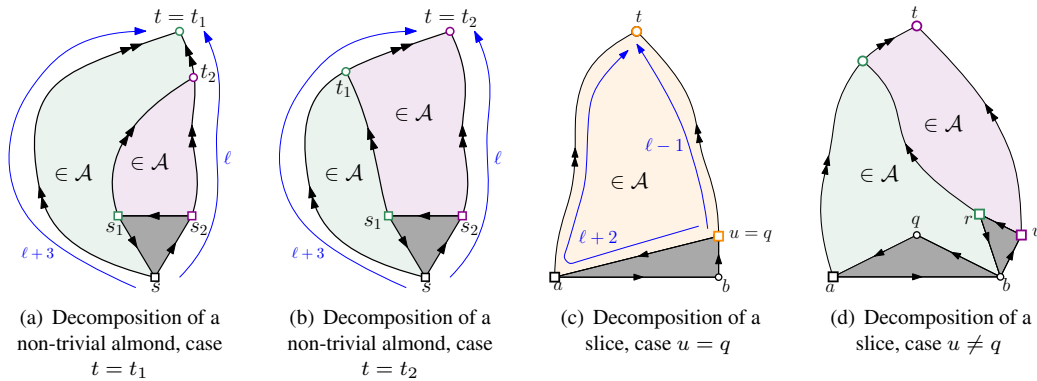


**Fig. 2:** Almond triangulations are elementary pieces for the algebraic decomposition of corner triangulations

Similarly we prove that  $t$  has only facial clockwise triangles: indeed a non-facial clockwise triangle in  $t$  should cross  $\gamma$ , hence have at least two vertices on  $\gamma$  and thus contain an inner edge of  $t_1$  or  $t_2$  with endpoints on  $\gamma_i$  as above.  $\square$

### 3.2 Almond triangulations

A corner quasi-triangulation with root vertex  $s$  is said to have an *apex*  $t$  if the boundary of its outer face consists of two paths from  $s$  to  $t$ , respectively called the left and right boundaries. Then a corner quasi-triangulation  $a$  with root vertex  $s$  and apex  $t$  is an *almond triangulation of height*  $\ell$  if its right boundary has length  $\ell$  and is the unique shortest path in  $a$  from  $s$  to  $t$ , while its left boundary has length  $\ell + 3$ .

Let  $\mathcal{A}$  be the family of almond triangulations, and let  $A(z) = \sum_{a \in \mathcal{A}} z^{n(a)}$ . Observe that there is exactly one almond triangulation  $a$  with  $n(a) = 0$ , called the *trivial almond*: it consists of a rooted white triangle with  $t = s$ . In order to prove Theorem 3 it is thus enough to prove the following:

**Proposition 10** *There is a bijection between non-trivial almond triangulations of size  $n$  and pairs of almond triangulations of total size  $n - 1$ .*

**Proof:** Let  $a$  be an almond of size  $n \geq 1$ , root  $s$ , apex  $t$ , and height  $\ell \geq 1$ . Let  $s_2$  be the endpoint of the root edge of  $a$ , and let  $s_1$  be the third vertex incident to the black face on the left of the root edge. Then  $s_1$  is at distance  $\ell + 1$  from  $t$ , because of the uniqueness of the shortest path from  $s$  to  $t$ . Consider  $\gamma$ , the leftmost shortest path from  $s_1$  to  $t$  that does not pass through  $s$ . Let  $t_1$  and  $t_2$  be the vertices where  $\gamma$  meets the left and right boundaries of  $a$ . Observe that at least one of the two equalities  $t_i = t$  occurs. Cutting  $a$  along  $\gamma$ , we get a black triangle  $(s, s_2, s_1)$  and two almonds with root vertex  $s_1$  and  $s_2$  and apex  $t_1$  and  $t_2$  respectively, see Fig. 2(a)-(b).

Conversely, let  $a_i, i = 1, 2$  be two almonds with root vertex  $s_i$ , apex  $t_i$ , and height  $\ell_i \geq 0$ . Let  $s$  and  $u$  be the second vertex on the left boundary of  $a_1$  and  $a_2$  respectively. We identify  $s_1$  and  $u$ , and glue the right boundary of  $a_1$  to the left boundary of  $a_2$ , edge by edge, up to the end of one of the two boundaries: this gluing path has length  $\ell_0 = \min(\ell_1, \ell_2 + 2)$ . Finally, we add a root edge  $(s, s_2)$ . According to Lemma 9, the resulting map  $b$  is a corner quasi-triangulation with an apex.

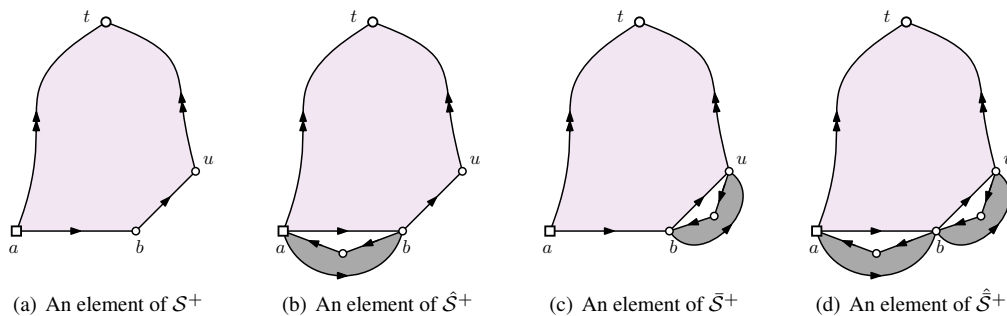


**Fig. 3:** The four types of maps of size  $n$  obtained from  $\mathcal{S}_n^+ \cup 2\mathcal{S}_{n-1}^+ \cup \mathcal{S}_{n-2}^+$ .

- If  $\ell_0 = \ell_1$ , then  $\mathfrak{b}$  has  $t_2$  for its apex, its right boundary has length  $1 + \ell_2$ , and its left boundary has length  $(\ell_1 + 2) + (\ell_2 + 2) - \ell_0 = \ell_2 + 4$ . Moreover, any path of length  $\ell_2 + 1$  from  $s$  to  $t_2$  uses the root edge (since  $s$  is at distance  $\ell_2 + 2$  from  $t_1$  in  $\mathfrak{a}_1$ ) and the shortest path is therefore unique since  $\mathfrak{a}_2$  is an almond. Hence  $\mathfrak{b}$  is itself an almond.
- If  $\ell_0 = \ell_2 + 2$ , then  $\mathfrak{b}$  has  $t_1$  for its apex, its left boundary has length  $\ell_1 + 2$ , and its right boundary has length  $1 + \ell_2 + \ell_1 - \ell_0 = \ell_1 - 1$ . The uniqueness property follows as above and  $\mathfrak{b}$  is an almond.

In both cases Lemma 9 ensures that the gluing path can be recovered as a leftmost shortest path in  $\mathfrak{b}$  after removing the root edge. This concludes the proof that the construction is bijective.  $\square$

### 3.3 Slices have algebraic generating series

A corner quasi-triangulation with root edge  $(a, b)$  and apex  $t$  is a *slice of height  $\ell$*  if its left and right boundaries are both shortest paths from  $a$  to  $t$ , while the path from  $b$  to  $t$  along the right boundary is the unique shortest path from  $b$  to  $t$  and has length  $\ell \geq 1$ .

Let  $\mathcal{S}^{(\ell)}$  be the set of the slices of height  $\ell$ ,  $\mathcal{S} = \bigcup_{\ell \geq 1} \mathcal{S}^{(\ell)}$  the family of the slices of positive height,  $\mathcal{S}_n = \{\mathfrak{p} \in \mathcal{S} \mid n(\mathfrak{p})\}$  the subset of slices with  $n$  black triangles and  $\mathcal{S}(z) = \sum_{\mathfrak{p} \in \mathcal{S}} z^{n(\mathfrak{p})}$  the generating function of slices. Then Formula (3) follows from the following proposition:

**Proposition 11** *There is a bijection between  $\mathcal{S}_{n-1} \cup \mathcal{S}_n$  and  $\mathcal{A}_{n-1} \cup (\mathcal{A}^2)_{n-2}$ , where  $(\mathcal{A}^2)_{n-2}$  denotes the set of pairs of elements of  $\mathcal{A}$  of total size  $n - 2$ .*

**Proof (sketch):** Let  $\mathfrak{p}$  be a slice with root edge  $e = (a, b)$ , and let  $\hat{\mathfrak{p}}$  be the map obtained from  $\mathfrak{p}$  by adding a new root edge  $\hat{e}$  parallel to  $e$  in the root face, and two triangles between  $e$  and  $\hat{e}$  (this new edge is parallel to  $e$  so that in particular  $\hat{\mathfrak{p}}$  is not a corner quasi-triangulation, see Fig. 3(b)). Let  $\hat{\mathcal{S}} = \{\hat{\mathfrak{p}} \mid \mathfrak{p} \in \mathcal{S}\}$ : elements of  $\hat{\mathcal{S}}$  of size  $n$  are in bijection with elements of  $\mathcal{S}$  of size  $n - 1$ . We prove Proposition 11 by describing a bijection between triangulations of  $\mathcal{S} \cup \hat{\mathcal{S}}$  with  $n$  black triangles and elements of  $\mathcal{A}_{n-1} \cup (\mathcal{A}^2)_{n-2}$ .

Consider indeed an element  $\mathfrak{p}$  of  $\mathcal{S}_n \cup \hat{\mathcal{S}}_n$  of height  $\ell$ . Let  $(a, b)$  be its root edge,  $q$  be the third vertex of the black face incident to it, and  $u$  be the vertex following  $b$  on the right boundary. There are two cases, as illustrated by Figure 2(c)-(d). If  $u = q$ , then  $\mathfrak{p} \in \mathcal{S}$  and  $\mathfrak{p}$  can be bijectively decomposed into a black face  $(a, b, q)$  and an almond with root vertex  $q$ , apex  $t$  and size  $n - 1$ . Otherwise, let  $r$  be the third vertex of the black face incident to  $(b, u)$ ;  $r$  is at distance  $\ell + 1$  from  $t$  (by uniqueness of the right boundary path).

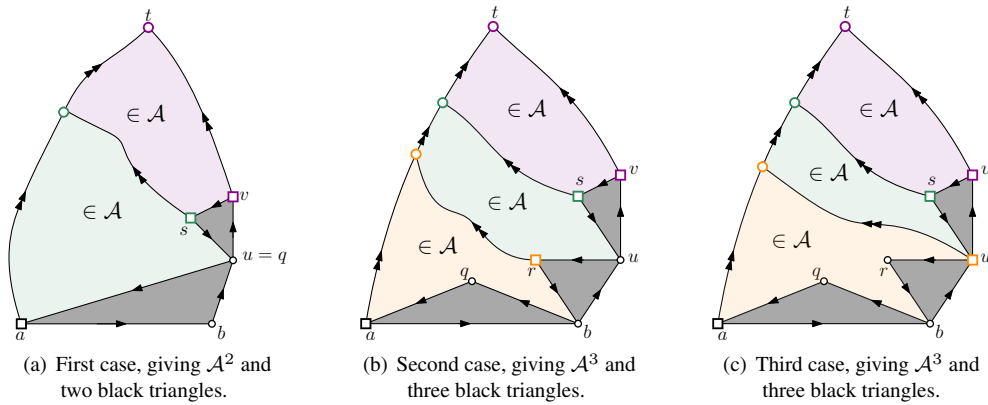


Fig. 4: The three cases in the decomposition of slices of height at least 2.

Consider the leftmost shortest path from  $r$  to  $t$  that does not pass through  $(b, u)$ . Then  $\mathfrak{p}$  can be bijectively decomposed into two black triangles  $(a, b, q)$  and  $(b, u, r)$ , and two almonds with respective root vertices  $r$  and  $u$  and total size  $n - 2$ , or, alternatively, into a black face  $(a, b, q)$  and a non-trivial almond with root vertex  $b$ , apex  $t$  and size  $n - 1$ .

□

### 3.4 Slices of height at least 2 have algebraic generating series

Let  $\mathcal{S}^+ = \mathcal{S} \setminus \mathcal{S}^{(1)}$  denote the set of slices of height at least 2. The following proposition yields a combinatorial proof of Formula (4):

**Proposition 12** *There is a bijection between  $\mathcal{S}_n^+ \cup 2\mathcal{S}_{n-1}^+ \cup \mathcal{S}_{n-2}^+$  and  $(\mathcal{A}^2)_{n-2} \cup 2(\mathcal{A}^3)_{n-3}$ .*

**Proof (sketch):** Let  $\mathfrak{p}$  be an element of  $\mathcal{S}^+$ , and define  $\hat{\mathfrak{p}}$  as in the previous section. Similarly, let  $\bar{\mathfrak{p}}$  be the map obtained from  $\mathfrak{p}$  upon adding a new edge and two triangles parallel to the edge following the root on the right boundary of  $\mathfrak{p}$ , see Fig. 3(c). Let then  $\hat{\mathcal{S}}^+ = \{\hat{\mathfrak{p}} \mid \mathfrak{p} \in \mathcal{S}^+\}$ ,  $\bar{\mathcal{S}}^+ = \{\bar{\mathfrak{p}} \mid \mathfrak{p} \in \mathcal{S}^+\}$  and  $\hat{\hat{\mathcal{S}}}^+ = \{\hat{\hat{\mathfrak{p}}} \mid \mathfrak{p} \in \mathcal{S}^+\}$ . Elements of  $\hat{\mathcal{S}}_n^+$  and  $\bar{\mathcal{S}}_n^+$  are in bijection with elements of  $\mathcal{S}_{n-1}^+$ , while elements of  $\hat{\hat{\mathcal{S}}}_n^+$  are in bijection with elements of  $\mathcal{S}_{n-2}^+$ . We prove Proposition 12 by describing a bijection between triangulations of  $\mathcal{S}^+ \cup \hat{\mathcal{S}}^+ \cup \bar{\mathcal{S}}^+ \cup \hat{\hat{\mathcal{S}}}^+$  with  $n$  black triangles and elements of  $(\mathcal{A}^2)_{n-2} \cup 2(\mathcal{A}^3)_{n-3}$ .

Consider indeed an element  $\mathfrak{p}$  of  $\mathcal{S}^+ \cup \hat{\mathcal{S}}^+ \cup \bar{\mathcal{S}}^+ \cup \hat{\hat{\mathcal{S}}}^+$  of height  $\ell \geq 2$ , and let the vertices  $a, b, u, q$  and  $r$  be defined as in the previous section. Let furthermore  $(u, v)$  be the edge following  $u$  on the right boundary of  $\mathfrak{p}$  and  $s$  be the third vertex of the incident black triangle, and  $\gamma_s$  and  $\gamma_u$  be the leftmost shortest paths from  $s$  (respectively  $u$ ) to  $t$  that do not pass through  $b$  nor  $(u, v)$ . There are three cases, illustrated by Figure 4. If  $u = q$  and  $\mathfrak{p} \in \mathcal{S}^+$ , then  $a = r$  and  $\gamma_u$  follows the left boundary. This leads to a decomposition of  $\mathfrak{p}$  into two black faces and two almonds with root vertex  $s$  and  $v$  and total size  $n - 2$ . Otherwise, cutting along  $\gamma_s$  and  $\gamma_u$  leads to a decomposition into three black faces and three almonds with total size  $n - 3$ . These almonds have root vertex  $s$  and  $v$ , and either  $r$  or  $u$  depending on the distance of  $r$  from  $t$ : if  $r$  is at distance  $\ell + 1$ , then  $r$  belongs to  $\gamma_u$  and is the root vertex of the third almond;

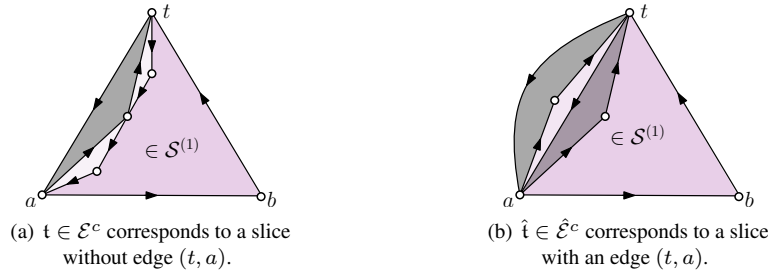


Fig. 5: Correspondence between corner triangulations and slices of height 1.

otherwise, that is if  $r$  is at distance  $\ell + 4$ , it does not belong to  $\gamma_u$ , and  $u$  is the root vertex of this third almond. Conversely, any three almonds with total size  $n - 3$  can be glued together in two ways with three additional black faces to produce an element of  $\mathcal{S}^+ \cup \hat{\mathcal{S}}^+ \cup \bar{\mathcal{S}}^+ \cup \tilde{\mathcal{S}}^+$ .  $\square$

### 3.5 Corner triangulations are slices of height 1

Formula (7) follows from the following proposition:

**Proposition 13** *There is a bijection between  $\mathcal{E}_{n-1}^c \cup \mathcal{E}_n^c$  and  $\mathcal{S}_{n-1}^{(1)}$ .*

**Proof:** For any element  $t$  of  $\mathcal{E}^c$ , let  $\hat{t}$  be defined as in Section 3.3, and  $\hat{\mathcal{E}}^c = \{\hat{t} \mid t \in \mathcal{E}^c\}$ . Then elements in  $\hat{\mathcal{E}}^c$  with  $n > 1$  black faces are in bijection with elements in  $\mathcal{E}^c$  with  $n - 1$  black faces. Now removing the root black triangle of elements of  $\mathcal{E}_n^c \cup \hat{\mathcal{E}}_n^c$  yields a slice of height 1 with  $n - 1$  black triangles, and this is clearly a bijection. There are two cases, illustrated by Figure 5.  $\square$

## 4 A non-recursive bijection between binary trees and almonds

The recursive decomposition of almond triangulations described by Proposition 10 clearly has the same structure as the root vertex deletion decomposition for rooted binary trees. This immediately yields a recursively defined bijection  $\varphi$  between rooted binary trees with  $n$  inner vertices and almonds with  $n$  black faces: if a binary tree  $b$  is reduced to a leaf then  $\varphi(b)$  is the only almond of size 0, that is, a rooted white triangle, and otherwise if  $b_1$  and  $b_2$  are the two subtrees of  $b$  at its root then  $\varphi(b)$  is the almond triangulation obtained upon gluing together  $\varphi(b_1)$  and  $\varphi(b_2)$  as in Proposition 10. The rest of this section is devoted to the alternative description of a direct construction of  $\varphi$ .

**From rooted binary trees to cacti** First observe that any rooted binary tree  $b$  with  $n$  nodes and  $n + 1$  leaves can be bijectively represented by a quasi-triangulation  $c = c(b)$  with  $n$  black and  $n + 1$  white triangular faces, called a *binary cactus*: each triangle of  $c$  corresponds to a vertex of  $b$ , and two triangles share a vertex if and only if the corresponding vertices are adjacent in  $b$ . Figure 6(a) shows a binary cactus and the underlying binary tree. By construction the only cycles of  $c$  are the triangular faces, and the boundary of the root face consists of the  $3n$  counterclockwise edges and  $3n + 3$  clockwise edges.

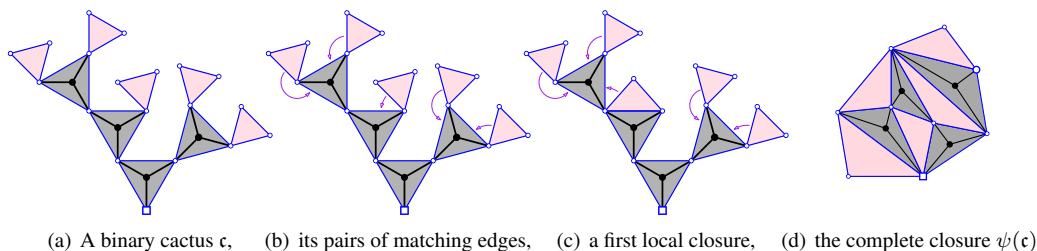


Fig. 6: The closure of binary cacti.

**The closure of a rooted cactus** In order to transform each binary cactus  $c$  into an almond  $a$  we construct iteratively a sequence of intermediary quasi-triangulations  $t_0 = c, t_1, \dots, t_k = a$ , by performing a sequence of local closure operations which we now describe. Let  $\mathcal{Q}_n$  denote the set of rooted quasi-triangulations with  $n$  black (counterclockwise) triangles and  $n + 1$  white (clockwise) triangles. In particular binary cacti and almonds with  $n$  black triangles belong to  $\mathcal{Q}_n$ .

Let  $t$  be an element of  $\mathcal{Q}_n$ . The counterclockwise traversal of the boundary of its root face starting at the root vertex leads to a sequence  $e_1, \dots, e_{2\ell+3}$  of oriented edges, for some  $\ell \geq 0$ , with  $\ell$  counterclockwise and  $\ell + 3$  clockwise edges. A pair  $(e_i, e_{i+1})$  is a pair of matching edges if  $e_i$  is clockwise and  $e_{i+1}$  is counterclockwise. The local closure of  $t$  at  $i$  is then the map obtained from  $t$  upon gluing  $e_i$  and  $e_{i+1}$ : in particular the sequence of its boundary edges is  $e_1, \dots, e_{i-1}, e_{i+2}, \dots, e_{2\ell+3}$ , see Fig. 6(c).

The local closure behaves exactly as standard parenthesis matching, with clockwise and counterclockwise edges playing respectively the role of opening and closing parenthesis: if  $t$  has two distinct pairs of matching edges and then the two local closure operations commute, and more generally the iteration of local closures until no pair of matching edges are left defines unambiguously the complete closure  $\psi(t)$  of the quasi-triangulation  $t$ , independantly of the order in which local closures are performed.

Let  $e_1, \dots, e_{2\ell+3}$  be the clockwise sequence of boundary edges of  $\psi(t)$ : since  $\psi(t)$  has no pair of matching edges, the first  $\ell$  edges  $e_1, \dots, e_\ell$  are counterclockwise and form a counterclockwise path from the root vertex  $s$  to a vertex  $t$ , while  $e_{2\ell+3}, \dots, e_{\ell+1}$  form a clockwise path from  $s$  to  $t$ . In particular the boundary of  $\psi(t)$  is compatible with it being an almond of height  $\ell$ .

**The complete closure is a bijection** This follows from the equality  $\psi \circ c = \varphi$ , which is easily proven by induction: if  $b$  is reduced to a leaf, then  $c(b)$  is a clockwise white triangle and  $\psi(c(b)) = c(b) = \varphi(b)$ . Otherwise let  $b_1$  and  $b_2$  denote the two subtrees of  $b$  at its root, and let  $a_1 = \varphi(b_1)$  and  $a_2 = \varphi(b_2)$ . By induction hypothesis,  $\psi(c(b_1)) = a_1$  and  $\psi(c(b_2)) = a_2$ . Now  $\psi(c(b))$  can be obtained by first performing the local closure inside the subtrees  $b_1$  and  $b_2$  to get a quasi-triangulation made of a black root triangle attached to  $a_1$  on the left hand side and  $a_2$  on the right hand side. The remaining local closures identify the right hand side of  $a_1$  with the left hand side of  $a_2$ : this is exactly equivalent to the gluing procedure of Proposition 10, and  $\psi(c(b)) = \varphi(b)$ .

## 5 Conclusion

In Eppstein and Mumford (2014), Theorem 1 is obtained in two steps: the authors first show that a cubic planar graph can be represented as a corner polyhedron if and only if its dual can be endowed with some

*cycle cover* structure; then they describe a constructive algorithm based on the decomposition into 4-connected components to prove that an Eulerian triangulation admits a cycle cover if and only if it is what we call here a corner triangulation.

It turns out that our bijection  $\psi$  can actually be slightly enhanced to produce directly an almond triangulation endowed with a certain  $\alpha$ -orientation of a derived map, equivalent to a cycle cover of the triangulation. This leads to an alternative algorithm for realizing a cubic planar graph as a corner polyhedron that does not involve its decomposition into 4-connected components: given a plane graph turn its dual triangulation into an almond using Proposition 13 and removing a black triangle, then decompose this almond into a binary tree using Proposition 10, and finally apply  $\psi$  to reform the almond now endowed with a cycle cover structure, and the associated triangulation.

This enhanced version of the complete closure also allows to prove directly that  $\psi$  is a bijection, without using Proposition 10. This approach is reminiscent of the proofs in Bernardi and Fusy (2012a,b, 2014), and strongly suggests that the master theorem of these papers could be nicely unified with a bicolored version of Bouttier and Guitter (2014).

## Acknowledgements

C. D. and G. S. wish to thank Simone Rinaldi for his hospitality in Siena university where part of this work was done.

## References

- M. Albenque and D. Poulalhon. A generic method for bijections between blossoming trees and planar maps. *Electron. J. Combin.*, 22(2):P2.38, 2015.
- C. Banderier, P. Flajolet, G. Schaeffer, and M. Soria. Planar maps and Airy phenomena. In *Proceedings of ICALP*, pages 388–402, 2000.
- O. Bernardi and E. Fusy. A bijection for triangulations, quadrangulations, pentagulations, etc. *J. Comb. Theory, Ser. A*, 119(1):218–244, 2012a.
- O. Bernardi and E. Fusy. Unified bijections for maps with prescribed degrees and girth. *J. Combin. Theory Ser. A*, 119(6):1352–1387, 2012b.
- O. Bernardi and E. Fusy. Unified bijections for planar hypermaps with general cycle-length constraints, 2014. arXiv:1403.5371.
- J. Bouttier and E. Guitter. On irreducible maps and slices. *Combinatorics, probabilities and computing*, 23:914–972, 2014.
- D. Eppstein and E. Mumford. Steinitz theorems for simple orthogonal polyhedra. *J. Computational Geometry*, 5(1):179–244, 2014.
- I. P. Goulden and D. M. Jackson. *Combinatorial Enumeration*. John Wiley, New York, 1983.
- G. Schaeffer. Planar maps. In *Handbook of enumerative combinatorics*. CRC Press, 2015.
- W. T. Tutte. A census of planar triangulations. *Canad. J. Math.*, 14:21–38, 1962.